Novel Dual-Band Quasi-0-dB Coupled-Line Coupler Using the Composite Right/Left-Handed Transmission Lines

Pei-Ling Chi, *Member, IEEE*, and Chun-Chih Liu

***Abstract*— A novel edge-coupled symmetric coupled-line coupler featuring the quasi-0-dB couplings at adjacently dual frequencies is presented based on the composite right/left-handed (CRLH) transmission lines. The fulfillment of dual-frequency quasi-0-dB couplings is derived from the complete backward and complete forward coupling phenomena at the higher and lower operating frequencies, respectively. To this end, the dispersion relations of the even and odd-mode CRLH lines have to be engineered in a particular manner so that: 1) the substantial attenuation level for each mode; 2) the 180° phase difference between the even and odd-mode reflection coefficients in the overlapped stopband region are obtained to accomplish the complete backward coupling; 3) the enabling curve intersection for the even and odd-mode Bloch impedances; and 4) the considerable difference between the even and odd-mode propagation constants in the left-handed regions are obtained to suppress the impedance coupling and attain strong forward coupling. Based on a thorough analysis on the even and odd-mode dispersion characteristics and Bloch impedances of the coupled lines, the operating principle and design procedure for the proposed coupler with dual-band complete couplings can be fully explained and greatly simplified. A symmetric CRLH coupled-line coupler consisting of seven coupled unit cells was experimentally developed and a shielding (metal) box was used to prevent radiation loss in the forward coupling band. Experimental results show that the maximum coupling levels are −1.3 and −0.9 dB, corresponding to the 3-dB fractional bandwidths of 15.8% and 10.8% at the lower and higher operating frequencies, respectively. Good agreement is obtained between the simulated and experimental results.**

***Index Terms*— Composite right/left-handed (CRLH), coupled-line coupler, dual-band, even and odd-mode, quasi-0-dB, transmission lines.**

I. Introduction

THE COUPLED-LINE couplers based on the edge-coupling scheme are well known for their limited coupling capability [1]. To achieve a tight coupling in the backward direction, a high impedance contrast between the even and odd-mode characteristic impedances is needed. Therefore, the backward coupling is mainly confined by the minimum achievable line gap and is accompanied by the unwanted forward coupling as the gap decreases [2]. In [3], a three-section coupled-line backward coupler was proposed to implement an arbitrary coupling coefficient. It was shown that, however, auxiliary approaches are required to realize a large even to odd-mode impedance ratio for a high coupling level. On the other hand, when strong forward coupling is preferred, an excessively long coupling length is required for developing a substantial phase difference between the even and odd-mode lines, and it can be shown that the coupling length for a complete forward coupling is on the order of several tens of wavelengths [4]. Therefore, a variety of approaches were reported to attempt an improved coupling level at the expense of the increased design/fabrication complexity [5], [6].

Recently, the coupled-line couplers based on the composite right/left-handed (CRLH) transmission lines [7]–[14] have successfully demonstrated the advantages of enhanced coupling ability and/or reduced coupler size. When operating in the left-handed region, the asymmetric coupler that comprises a CRLH transmission line pairing with a microstrip line is able to exhibit strong backward coupling [7], [8]. On the other hand, the symmetric couplers can be applied to implement tight backward or forward coupling depending on the operational regions. In particular, when the even and odd-mode lines operate in a stopband, the coupling strength relies on the attenuation length of the coupled section and is able to present 3-dB backward coupling [9] and up to the complete backward coupling [10] at a reduced coupling length and a relaxed line gap. In addition, the enhanced forward coupling was implemented by engineering the pair of dispersion relations such that the even and odd-mode propagation constants is developed with an appreciable difference in the left-handed region [11], [12]. The overview of a generalized coupled-line coupler, including the conventional symmetric or asymmetric, the CRLH symmetric or asymmetric, and the conventional-CRLH asymmetric prototypes, was given with the analytical formulations to examine the coupling phenomenon and explain the underlying operating theory [14]. So far, less effort has been made to develop an edge-coupled coupled-line coupler that shows the capability of dual complete couplings at frequencies of interest.

In this paper, a symmetric and edge-coupled CRLH coupler designed for complete couplings in dual bands was carried out and analyzed by the even and odd-mode decomposition technique. In spite of applying similar design concepts for the coupling enhancement in the backward (contra-directional)

Manuscript received August 18, 2013; revised November 27, 2013; accepted December 9, 2013. Date of publication January 9, 2014; date of current version January 30, 2014. This work was supported by the National Science Council of Taiwan under Grant NSC 101-2221-E-009-108 and Grant NSC 102-2221-E-009-029. Recommended for publication by Associate Editor Y.-L. Li upon evaluation of reviewers' comments.

The authors are with the Electrical and Computer Engineering Department, National Chiao Tung University, Hsinchu 300, Taiwan (e-mail: peilingchi@nctu.edu.tw; peiling@ee.ucla.edu).

Color versions of one or more of the figures in this paper are available online at http://ieeexplore.ieee.org.

Digital Object Identifier 10.1109/TCPMT.2013.2295920

[10] and forward (co-directional) [11], [12] directions, to fulfill the complete couplings at dual frequencies, it will be discussed that the dispersion relations as well as the Bloch impedances of the even and odd-mode lines must be tailored in a particular manner, which was not emphasized in the former studies where only single-band operation is concerned [7]–[14]. In particular, the presented analysis of the even and odd-mode Bloch impedances will lead to the same solution of the even and odd-mode dispersion relations as applied in [10] where such a discussion was not given theoretically. Thus, the design procedure shown here is very useful to simplify development of the complete couplings in dual bands. The even and odd-mode dispersion relations are engineered in a fashion that an overlapped stopband region at a higher frequency is designed for complete backward coupling, and meanwhile, the left-handed phase difference in the lower band is enlarged to a large degree for implementation of the complete forward coupling. As will be addressed that by decreasing the distance between the pair of shorting vias in a coupled unit cell, the phase difference of the even and odd-mode lines can be considerably increased to reduce the coupler length. Note that the tradeoff between the backward coupling performance, including the coupling level and bandwidth, and the attainable difference in the even- and odd-mode propagation constants, which determines the coupler length, was carefully considered for the prototype design.

In this paper, a dual-band quasi-0-dB coupled-line coupler consisting of seven CRLH coupled unit cells was implemented and characterized experimentally. The dual-band impedance matching was carried out using the tapered microstrip section at each port. In addition, a metal or shielding box was designed to prevent the fast-wave radiation loss in the forward coupling region. This paper is organized as follows. In Section II, the operating principle and design procedure of the dual-band complete coupling coupler are discussed by the analysis on the even and odd-mode dispersion relations and Bloch impedances. In Section III, the dispersion engineering technique is applied to develop the coupler prototype. To start with, the coupled unit cell was properly designed to achieve the desired frequency behavior. A comprehensive parametric study was conducted to find an optimal/compromise solution for the complete couplings at dual frequencies. In Section IV, the full-wave simulated results of the entire structure are presented and compared with the experimental data. Good agreement is obtained.

II. Operating Principle and Design Procedure for the Dual-Band Complete Coupling Coupler

A. Even and Odd-Mode Dispersion Relations and Bloch Impedances of the CRLH Coupled Line

Fig. 1 shows the configuration of the proposed dual-band quasi-0-dB coupled-line coupler inside a metal box. The port designation is defined in the same figure. Without loss of generality, if port 1 is the excitation port, ports 2–4 are the through, backward coupled, and forward coupled ports, respectively. Due to the symmetric property, the even and odd-mode decomposition is applied to analysis of the

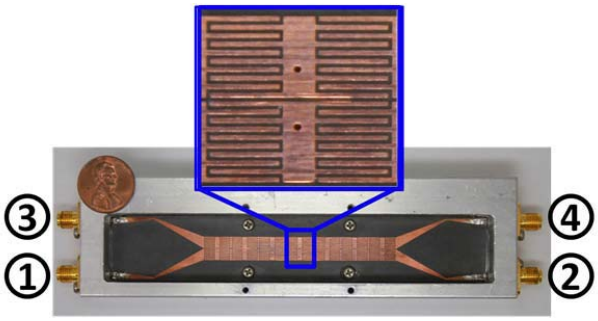

Fig. 1. Proposed dual-band quasi-0-dB coupled-line coupler. The coupled unit cell is magnified in the inset.

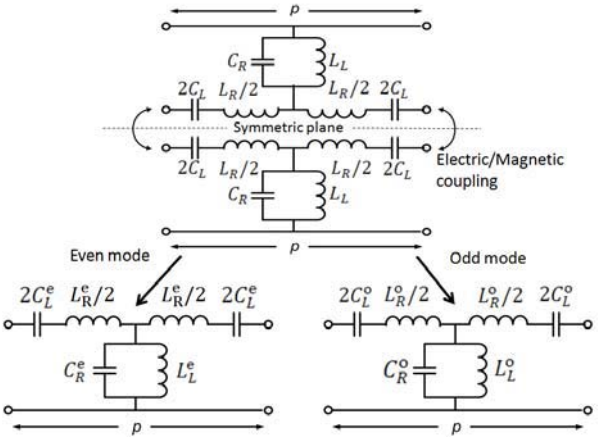

Fig. 2. Even and odd-mode equivalent circuit models of the CRLH coupled line.

presented coupler. As shown in Fig. 2, under the even or odd-mode excitation, the symmetric plane of the coupled CRLH line is equivalent to a magnetic or electric wall, respectively. To consider the coupling effect, an equivalent mutual inductance or a coupling capacitance is used to represent the magnetic or electric coupling, and is included in the series inductance L_R^e of the even mode or in the shunt capacitance C_R^o of the odd mode, respectively. Thus, in either mode the resulting circuit model has the typical lumped components of a CRLH unit cell and thus the even or odd-mode line behaves as a CRLH line. In particular, the series capacitance C_L^i and shunt inductance L_L^i contribute to the left-handed properties of the artificial structure, while the series inductance L_R^i and shunt capacitance C_R^i represent the parasitic effects of the structure and the coupling phenomena between the two lines, where $i = e$ or o.

The implementation of dual-band complete couplings is best undertaken through the analysis and design on the even and odd-mode dispersion relations and Bloch impedances. In general, the even or odd-mode dispersion relation of the CRLH coupled line exhibits the unbalanced property with a stopband gap to separate the lower left-handed and the upper right-handed regions. Such an example is shown in Fig. 3 where the series and shunt resonant frequencies $\omega_{\rm se}^i$ and $\omega_{\rm sh}^i$ delimit the stopband region. The frequency range between the $\min(\omega_{\rm se}^i, \omega_{\rm sh}^i)$ and the left-handed cutoff frequency $\omega_{\rm cL}^i$

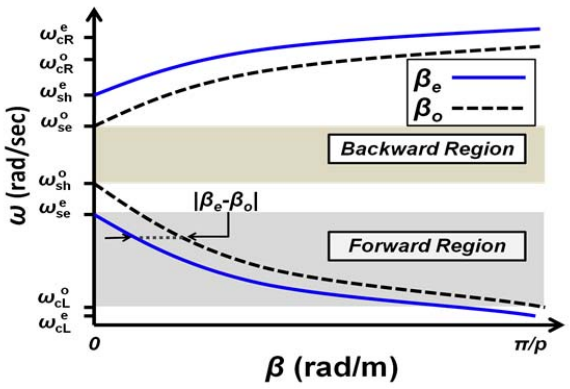

Fig. 3. Dispersion diagram of the CRLH even and odd-mode lines with $\omega^o_{\rm sh} > \omega^e_{\rm se}$.

is defined as the left-handed passband while the right-handed passband starts from the frequency $\max(\omega^i_{\rm se}, \omega^i_{\rm sh})$ to the right-handed cutoff frequency ω^i_{cR}, where the $\min(\omega^i_{\rm se}, \omega^i_{\rm sh})$ or $\max(\omega^i_{\rm se}, \omega^i_{\rm sh})$ stands for the minimum or the maximum frequency of the two frequencies $\omega^i_{\rm se}$ and $\omega^i_{\rm sh}$, respectively. By applying the transmission line theory to the even or odd-mode circuit model, the complex propagation constant γ_i can be obtained as follows [4]:

$$\gamma_i = j\omega\sqrt{L^i_R C^i_R\left[1-\left(\frac{\omega^i_{\rm se}}{\omega}\right)^2\right]\left[1-\left(\frac{\omega^i_{\rm sh}}{\omega}\right)^2\right]}, \quad i = e,\ o \tag{1}$$

where the series and shunt resonant frequencies are defined as follows:

$$\omega^i_{\rm se} = \frac{1}{\sqrt{L^i_R C^i_L}},\ \omega^i_{\rm sh} = \frac{1}{\sqrt{L^i_L C^i_R}}, \quad i = e,\ o. \tag{2}$$

At the meantime, the Bloch impedances of the even and odd-mode lines need to be studied, as will be used for impedance matching in dual bands. The Bloch impedance $Z_{\rm Bi}$ represents the practical impedance used for matching of the periodic structure and is given as follows [4]:

$$Z_{\rm Bi} = \sqrt{\frac{L^i_L}{C^i_L}}\sqrt{\frac{\left(\frac{\omega}{\omega^i_{\rm se}}\right)^2-1}{\left(\frac{\omega}{\omega^i_{\rm sh}}\right)^2-1}-\frac{\left[\left(\frac{\omega}{\omega^i_{\rm se}}\right)^2-1\right]^2}{4\omega^2 L^i_L C^i_L}}, \quad i = e,\ o. \tag{3}$$

From (3), it is clear that the series and shunt resonant frequencies $\omega^i_{\rm se}$ and $\omega^i_{\rm sh}$ correspond to the zero and pole frequencies, respectively. Moreover, the Bloch impedance is purely real in the right- and left-handed (passband) regions while being purely imaginary in the stopband. In particular, in the stopband $Z_{\rm Bi}$ is an inductive reactance when $\omega^i_{\rm se} < \omega^i_{\rm sh}$, and is a capacitive reactance when $\omega^i_{\rm se} > \omega^i_{\rm sh}$. This important property will be used later for impedance matching in a stopband for complete backward coupling. Fig. 4 shows the frequency behavior of the Bloch impedances $Z_{\rm Be}$ and $Z_{\rm Bo}$ in the right- and left-handed (passband) regions and in the stopband region. Note that the

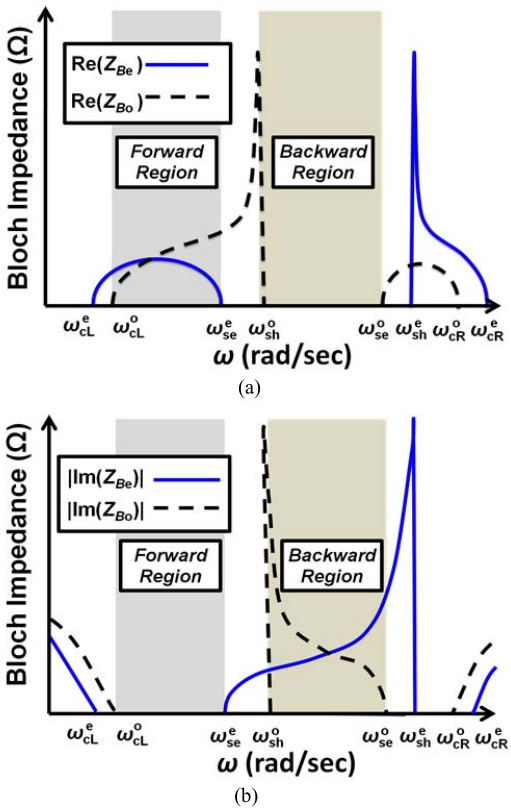

Fig. 4. Illustration of the even and odd-mode Bloch impedances of the CRLH coupled line with the corresponding dispersion relations in Fig. 3. (a) Passband and (b) stopband even and odd-mode impedances.

corresponding dispersion diagram was shown in Fig. 3. For the even-mode line, $\omega^e_{\rm sh} > \omega^e_{\rm se}$, whereas $\omega^o_{\rm sh} < \omega^o_{\rm se}$ for the odd-mode line. The detailed derivation and discussion for implementation of the complete backward and forward couplings in the respective bands will be given in the following.

B. Design Concept and Implementation of the Dual-Band Complete Backward and Forward Couplings

As shown in Figs. 3 and 4, the overlapped stopband region (the frequency range between $\omega^o_{\rm sh}$ and $\omega^o_{\rm se}$) of the even and odd-mode lines is the operational band used to implement complete backward coupling, while the left-handed passband region (the frequency range between $\omega^o_{\rm cL}$ and $\omega^e_{\rm se}$) is designed with enhanced difference in the even and odd-mode phase constants for complete forward coupling. Based on the even and odd-mode decomposition analysis, the S-parameters of the coupled-line coupler can be reconstructed from the two-port reflection coefficients S_{11e}/S_{11o} and transmission coefficients S_{21e}/S_{21o} of the even and odd-mode lines, as shown in [10]. To realize the impedance matching to the port termination Z_0, typically 50 Ω, the input impedances of the even and odd-mode lines have to satisfy the relation as follows:

$$Z_0 = \sqrt{Z_{{\rm in},e} Z_{{\rm in},o}}. \tag{4}$$

In a stopband, where the phase constants vanish ($\beta_e = \beta_o = 0$) and the attenuation lengths are assumed to be sufficiently large

($\alpha_e l, \alpha_o l \gg 1$, l is the coupler length), the input impedances $Z_{\text{in},e}^{\text{BW}}$ and $Z_{\text{in},o}^{\text{BW}}$ for backward coupling can be approximated as

$$Z_{\text{in},e}^{\text{BW}} \cong Z_{\text{Be}}^{\text{BW}} = jX_{\text{Be}}, \quad Z_{\text{in},o}^{\text{BW}} \cong Z_{\text{Bo}}^{\text{BW}} = jX_{\text{Bo}} \tag{5}$$

where the even and odd-mode Bloch impedances are reduced to the reactances X_{Be} and X_{Bo}, respectively, in a stopband. It follows that the matching condition for stopband operation can be derived as follows:

$$Z_0 \cong \sqrt{jX_{\text{Be}} \cdot jX_{\text{Bo}}}. \tag{6}$$

Thus, to achieve impedance matching for the backward coupling, the reactances X_{Be} and X_{Bo} have to be one positive (inductive) and the other one negative (capacitive), which can be realized by allocating the pair of the odd-mode resonant frequencies ω_{sh}^o and ω_{se}^o in inverted frequency order with respect to the even-mode counterpart, as shown in Fig. 4 where $\omega_{\text{sh}}^o < \omega_{\text{se}}^o$ and $\omega_{\text{se}}^e < \omega_{\text{sh}}^e$. Note that, once the input port is matched, all the power will be delivered to port 3 (the backward coupled port) in that the transmission coefficients of the even and odd-mode lines $S_{21\text{e}} = S_{21\text{o}} = 0$ in the stopband. Thus, the complete backward coupling can be realized at the higher frequency of the dual-band operation. Furthermore, it was concluded in [10] by simulation results that the even and odd-mode reflection coefficients, S_{11}^e and S_{11}^o, must be out of phase in the stopband for complete backward coupling. This result can be easily proved here as a consequence by applying the impedance matching condition in (6)

$$\left|\angle S_{11e}^{\text{BW}} - \angle S_{11o}^{\text{BW}}\right| \cong 2\left|\tan^{-1}\left(\frac{X_{\text{Bo}}}{Z_0}\right) - \tan^{-1}\left(\frac{X_{\text{Be}}}{Z_0}\right)\right| = \pi. \tag{7}$$

In the lower band, when the forward coupling is attempted in the left-handed (passband) regions of the even and odd-mode lines, given that the input port is matched ($S_{11} = 0$) and backward coupling is completely suppressed ($S_{31} = 0$), the complete forward coupling occurs when the phase constants of the even and odd modes satisfy the relation as follows:

$$(\beta_e - \beta_o)l = (\beta_e - \beta_o)\, p \cdot N = \pi \tag{8}$$

where p is the physical length of the unit cell and N is the number of coupled unit cells in the coupler. Thus, to reduce the coupler length, the phase difference from a unit cell, $(\beta_e - \beta_o) \cdot p$, should be increased as large as possible by proper dispersion engineering of the left-handed branches of the even and odd-mode lines, as shown in Fig. 3. However, as can be expected from Fig. 3, the increase in $|\beta_e - \beta_o|$ will lead to bandwidth reduction of the backward coupling region and deteriorate the backward coupling level as a result. Thus, a compromise needs to be made and will be examined in details in the next section. Similarly, to achieve input matching and suppress the backward coupling, i.e., $S_{11} = S_{31} = 0$, the Bloch impedances $Z_{\text{Be}}^{\text{FW}}$ and $Z_{\text{Bo}}^{\text{FW}}$ of the even and odd-mode lines have to match the port impedance as follows:

$$Z_0 = Z_{\text{Be}}^{\text{FW}} = Z_{\text{Bo}}^{\text{FW}}. \tag{9}$$

To this end, the Bloch impedances under consideration should exhibit the frequency responses, as the one shown in Fig. 4(a) where the passband resistances intersect at a frequency in the forward coupling region. If instead, the resonant frequencies ω_{se}^e of the even-mode line and ω_{sh}^o of the odd-mode line are designed such that $\omega_{\text{sh}}^o < \omega_{\text{se}}^e$, as shown in Fig. 5, the impedance coupling to port 3 will take place. Thus, by letting the two resonant frequencies as $\omega_{\text{se}}^e < \omega_{\text{sh}}^o$, the backward coupling in the lower operational band can be effectively suppressed and the tapered spacing lines toward the termination ports [15] can be removed with this regard.

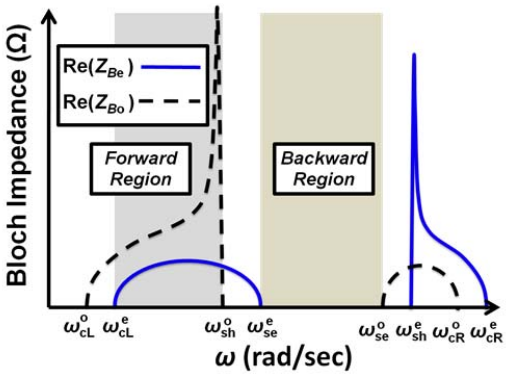

Fig. 5. Bloch impedances of the CRLH even and odd-mode lines for the case $\omega_{\text{se}}^e > \omega_{\text{sh}}^o$. Only the passband impedances are considered here.

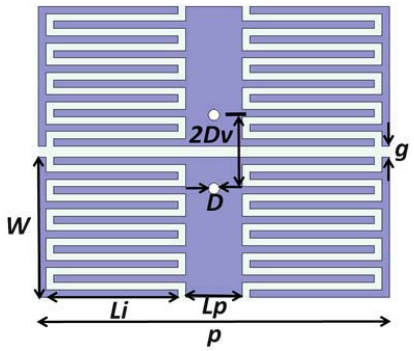

Fig. 6. Configuration of the coupled unit cell for the proposed dual-band quasi-0-dB coupler. The structural parameters are as follows: $D_v = 1.35$ mm, $D = 0.3$ mm, $g = 0.2$ mm, $W = 3.8$ mm, $L_p = 1.5$ mm, $L_i = 3.5$ mm, $p = 9.3$ mm, and the width of the digits and spacing are all 0.2 mm.

Based on all the aforementioned design considerations, a desired dispersion diagram of the even and odd-mode lines is shown in Fig. 3. Note that because of the inductive or capacitive coupling in the even or odd-mode excitation, the equivalent mutual inductance and coupling capacitance will contribute to the series inductance L_R^e of the even mode and the shunt capacitance C_R^o of the odd mode, respectively. Therefore, the relations of the resonant frequencies $\omega_{\text{se}}^e < \omega_{\text{sh}}^e$ and $\omega_{\text{sh}}^o < \omega_{\text{se}}^o$ in Fig. 3 can be easily carried out in practice.

III. Design of the CRLH Coupled-Line Coupler

A. Structure of the Proposed CRLH Coupled-Line Coupler

Fig. 6 shows the CRLH coupled unit cell for the proposed dual-band quasi-0-dB coupler. For each isolated unit cell, the interdigital capacitors and the shorting via contribute to the series capacitance and the shunt inductance in the

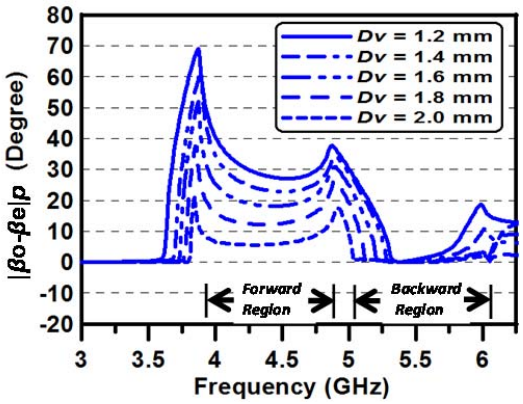

Fig. 7. Even and odd-mode phase difference with respect to the distance between the shorting vias in a coupled unit cell. The structural parameters are as follows: $D = 0.3$ mm, $g = 0.2$ mm, $W = 3.8$ mm, $L_p = 1.5$ mm, $L_i = 3.5$ mm, $p = 9.3$ mm, and the width of the digits and spacing are all 0.2 mm.

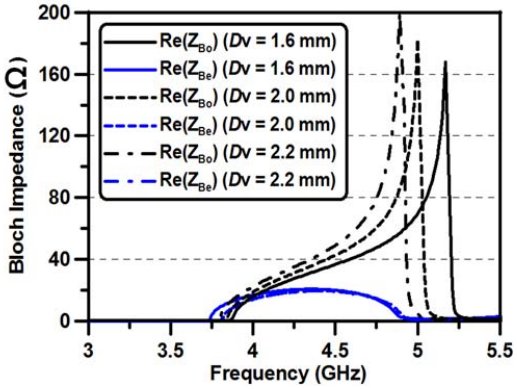

Fig. 8. Even and odd-mode passband (left-handed region) Bloch impedances with respect to the distance between the shorting vias in a coupled unit cell. The structural parameters as follows: $D = 0.3$ mm, $g = 0.2$ mm, $W = 3.8$ mm, $L_p = 1.5$ mm, $L_i = 3.5$ mm, $p = 9.3$ mm, and the width of the digits and spacing are all 0.2 mm.

equivalent circuit model, respectively. In addition, the parasitic effects induced by the current flow in metal patterns and the voltage difference between the metal and ground planes will produce the effective series inductance and shunt capacitance, respectively. The prototype of the unit cell was developed on a Rogers RT/Duroid substrate with the dielectric constant of 2.2 and the thickness of 1.58 mm. Since the radiation phenomenon is expected in the left-handed regions (the lower operational band) where the propagation constants β_e and β_o are less than the free space wave number (the fast-wave region in Fig. 9), the shielding box made of aluminum is used to suppress the radiation. Therefore, the dimensions of the metal box must be carefully designed so that the cutoff frequency of the lowest cavity mode is high enough to avoid the mode disturbances in the operational bands.

As observed in Fig. 6, the interdigital capacitors and the shorted strip (with strip width L_p) in the center are mainly used to control the operating bands. Furthermore, the distance between the pair of shorting vias in a coupled unit cell, $2 \times Dv$, is able to considerably increase the phase difference between the even and odd-mode lines, $|\beta_e - \beta_o| \cdot p$, and thus reduce the coupling length l $(= p \cdot N)$ required for complete forward coupling. Fig. 7 shows the study on the even and odd-mode phase difference with respect to the via-distance. It can be observed that as the via-distance decreases, the even and odd-mode phase difference of a coupled unit cell is conspicuously increased in the forward coupling region, and is ascribed to the increase of the odd-mode shunt resonant frequency $\omega^o_{\rm sh}$ and thus extends the difference gap between the left-handed branches when referring to the dispersion diagram in Fig. 3. This inference can be clearly observed in Fig. 8, where the odd-mode pole frequency $(\omega^o_{\rm sh})$ in the upper end of the left-handed passband is appreciably increased in association with a nearly unchanged zero frequency $(\omega^e_{\rm se})$ of the even mode as the via-distance decreases. In the meantime, the intersection point of the even and odd-mode Bloch impedances moves upward to the center of the forward coupling band, which is able to improve the isolation level in the backward direction.

On the other hand, in the higher operational band where the complete backward coupling is attempted, the adverse effect is returned as the via-distance decreases (or the even and odd-mode phase difference increases). As Dv varies from 2.0 to 1.2 mm in Fig. 7, the overlapped stopband bandwidth (with zero phase difference) decreases, which lessens the attenuation ability in the stopband. As discussed in Section II-B, the property of sufficient stopband attenuation is critical for complete backward coupling. Thus, the backward coupling level, bandwidth, and isolation level (for the forward coupling), will degrade accordingly in the higher band.

For better clarity, the performance comparison for the dual-band complete coupling couplers consisting of different numbers of coupled unit cells is summarized in Table I. Note that the cases of 4, 7, 10, and 14 unit cells are studied and each number is determined by the resulting phase difference given a corresponding via distance. In Table I, the isolation is defined as the backward or forward coupling level in the complete forward or backward coupling region, respectively. Due to application of the metal box for radiation suppression, it should be mentioned that the excitation of the cavity mode is observed in the backward coupling region when up to 10 unit cells are used, revealing that a smaller number of unit cells should be considered. As the number of unit cells varies, the performance tradeoff between the forward and backward coupling bands indicates that a compromise is needed and the case of seven unit cells is chosen as the coupler prototype for the dual-band complete couplings.

B. Even and Odd-Mode Analysis

The even and odd-mode decomposition was applied to analysis of the proposed symmetric and dual-band coupler. The full-wave calculated dispersion curves of the even and odd-mode lines are shown in Fig. 9. Note that the conductor and dielectric losses were included in the full-wave simulations. For the even mode, the left-handed region ranges from 3.8 to 4.8 GHz, and the stopband is from 4.8 to 6 GHz with the series resonant frequency $\omega^e_{\rm se}$ and the shunt resonant frequency

TABLE I
PERFORMANCE COMPARISON WITH DIFFERENT NUMBERS OF COUPLED UNIT CELLS

Number of Coupled Cells	4 cells (Dv = 0.85 mm)		7 cells (Dv = 1.35 mm)		10 cells* (Dv = 1.75 mm)		14 cells* (Dv = 1.95 mm)	
Coupling Region	Forward	Backward	Forward	Backward	Forward	Backward	Forward	Backward
Operating Frequency	4.34 GHz	5.89 GHz	4.55 GHz	5.8 GHz	4.43 GHz	5.44 GHz	4.44 GHz	5.3 GHz
Maximum Coupling Level	-0.41 dB	-3.0 dB	-0.6 dB	-0.4 dB	-0.85 dB	-0.25 dB	-1.09 dB	-0.25 dB
3-dB Bandwidth	24.2 %	14.1 %	18.4 %	14 %	> 17.8 %	16.4 %	13.8 %	20.5 %
Isolation Bandwidth (< -15 dB)	13.2 %	N.A.	15.7 %	10.9 %	7 %	15.6 %	2.0%	17.4 %
Dual-Band Separation	1.55 GHz		1.25 GHz		1.01 GHz		0.86 GHz	

* indicates that the cavity mode has been observed in the backward coupling region.

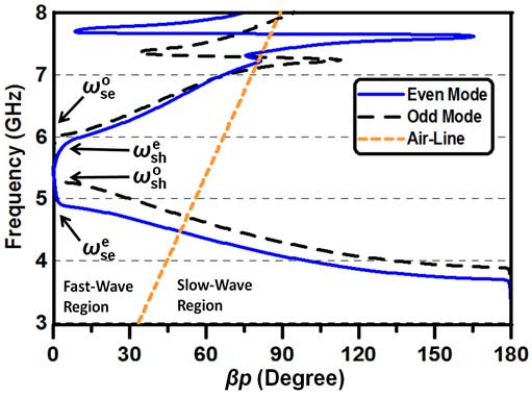

Fig. 9. Full-wave (HFSS) calculated dispersion diagram of the even and odd-mode lines for the proposed coupler.

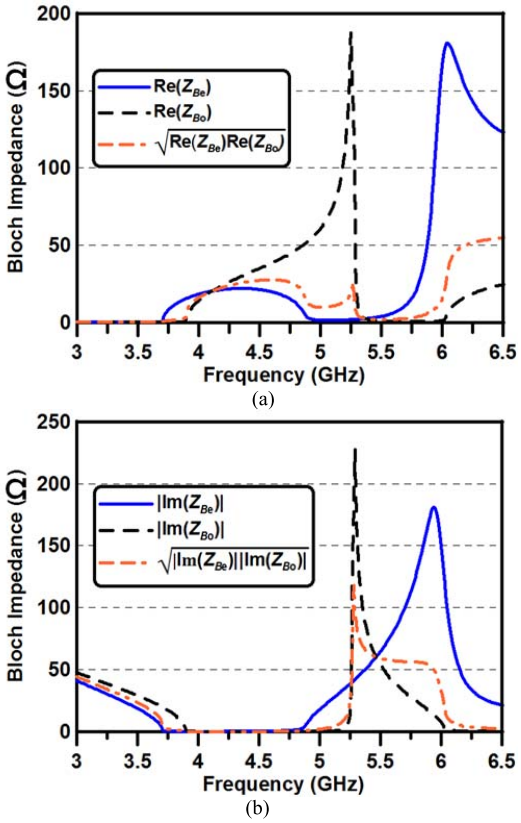

Fig. 10. Full-wave calculated Bloch impedances of the even and odd-mode lines for the proposed coupler. (a) Passband and (b) stopband impedances and the geometric mean.

ω_{sh}^{e} at 4.8 and 6 GHz, respectively. On the other hand, the left-handed and the stopband regions of the odd mode start from 3.95 to 5.3 GHz and from 5.3 to 6 GHz, respectively. The odd-mode shunt resonant frequency ω_{sh}^{o} is at 5.3 GHz while its series resonant frequency ω_{se}^{o} is at ~6 GHz. The prototype of the coupled unit cell was carefully designed so that both a considerable phase difference $|\beta_e - \beta_o| \cdot p$ in the left-handed region and a substantial overlapped stopband bandwidth were obtained. Note that the radiation phenomenon will take place in the left-handed passband to the left of the air line (the fast-wave region) and thus a metal box was used, in the design phase and the experimental implementation, to suppress the radiation loss in the forward coupling band.

As can be read in Fig. 7, in the case of $Dv = 1.4$ mm, the phase difference is about 25° per unit cell, thus requiring seven unit cells to realize the complete forward coupling. The even and odd-mode Bloch impedances for the proposed coupled lines are shown in Fig. 10. In the forward coupling region where both modes operate in the left-handed passbands, the Bloch impedances are real and intersect at 4.15 GHz. For maximum coupling bandwidth, the geometric mean impedance of 28 Ω is used for impedance matching in the lower band of the dual-band operation. On the other hand, the overlapped stopband of the even and odd-mode lines is employed for complete backward coupling, and thus the geometric mean of 55 Ω from the imaginary Bloch impedances is used herein.

Based on the calculated dispersion relations in Fig. 9, the equivalent even and odd-mode circuit models were extracted. Fig. 11 shows the calculated S-parameters of the even and odd-mode transmission lines, each consisting of seven unit cells, using the circuit simulations and the full-wave simulations. The extracted parameters for the even and odd-mode circuit models are given in the caption. As observed, good agreement is obtained. Since the circuit simulations are based on seven cascaded lumped cells, each with the constitutive parameters extracted from a single coupled unit cell, the interaction between the adjacent unit cells, in fact, is not considered and leads to the frequency shifts as compared with the counterparts from full-wave simulations. Moreover, the discrepancy observed at frequencies higher than the stopband of each mode is resulted from the extraction error of the circuit parameters, which were optimized for approximating the full-wave dispersion relation in dual bands of interest. From Fig. 11, it is clear that the even and odd-mode lines

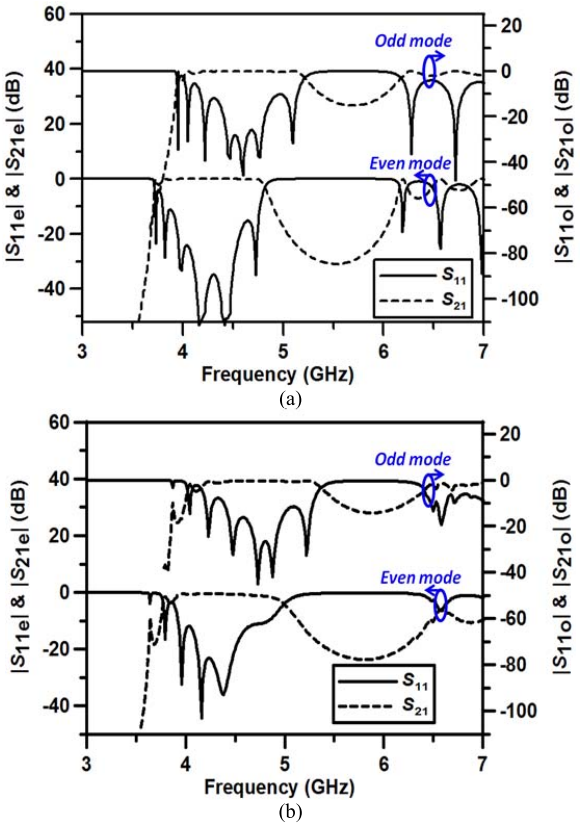

Fig. 11. Calculated S-parameters of the even and odd-mode lines composed of seven unit cells. (a) Circuit simulation results based on the extracted circuit parameters: $L_R^e = 3.72$ nH, $C_R^e = 1.8$ pF, $L_L^e = 0.42$ nH, $C_L^e = 0.29$ pF, $L_R^o = 2.42$ nH, $C_R^o = 2.16$ pF, $L_L^o = 0.41$ nH, and $C_L^o = 0.29$ pF. (b) Full-wave simulation results.

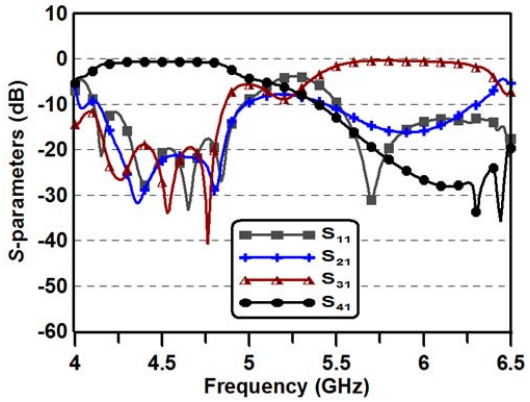

Fig. 12. Calculated S-parameters of the dual-band complete coupling coupler reconstructed from the full-wave S-parameters of the even and odd-mode lines in Fig. 11(b).

exhibit the unbalanced properties as required for this coupler. The even-mode series resonant frequency ω_{se}^e (at lower end of the stopband) is considerably lower than the odd-mode shunt resonant frequency ω_{sh}^o, which enlarges the difference gap between the even and odd-mode phase constants. In Fig. 12, the S-parameters of the coupled-line coupler are reconstructed from the prior full-wave simulated results of the even and odd-mode lines in Fig. 11(b). Note that to achieve dual-band

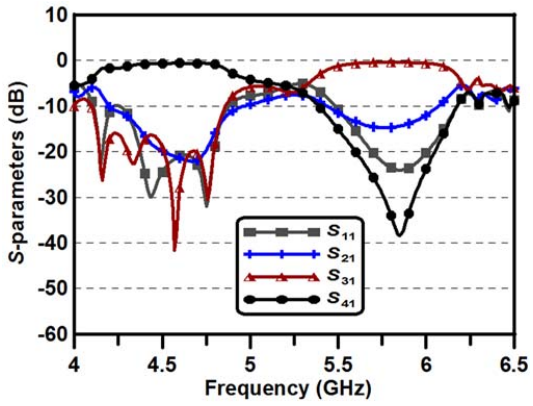

Fig. 13. Full-wave simulated S-parameters of the proposed dual-band quasi-0-dB coupled-line coupler.

impedance matching to 50 Ω, the ideal tapered line was used at each port in Fig. 12. Based on the numerical prediction of the even and odd-mode Bloch impedances, the tapered feed line was designed to match the geometric means of 28 and 55 Ω in the forward and backward coupling bands, respectively, to the 50-Ω termination. The dual-band complete couplings are obtained as desired. In particular, the maximum forward coupling occurs at 4.45 GHz with the coupling level of −0.65 dB while the maximum backward coupling takes place at 5.76 GHz with the coupling level of −0.43 dB. The 3-dB bandwidth of the forward coupling region is from 4.06 to 4.95 GHz and that of the backward coupling region is from 5.4 to 6.39 GHz, corresponding to the fractional bandwidths of 19.8% and 16.8%, respectively.

IV. Simulated and Experimental Results of the Dual-Band Quasi-0-dB Coupler

The full-wave analysis of the proposed coupler was conducted by the simulation tool, high frequency structure simulator (HFSS). The entire structure, including the CRLH coupled lines, the microstrip tapered sections that connect the coupled lines to the 50-Ω ports, and the metal box, was considered for the simulation model. To improve the prediction accuracy, the dielectric, conductor, and connector losses, were taken into consideration and moreover, the excitation type of wave port was assigned to each port of the coupler. The Rogers RT/Duroid substrate with the dielectric constant of 2.2 and the thickness of 1.58 mm was used to develop the coupler. To implement dual-band impedance matching, the tapered microstrip sections were used and due to the close distance between the coupled CRLH lines, the tapered spacing lines were applied to reduce the coupling between the pair of feed lines and thus avoid the introduction of additional even and odd-mode phase difference. Fig. 13 shows the full-wave simulation results for the proposed coupler where the dual-band operation of the quasi-0-dB coupling is observed. The lowest cavity mode that results from the metal box is at ∼6.3 GHz, which is away from the dual bands of interest and thus will not affect the coupler performance. The maximum forward coupling occurs at 4.55 GHz with a coupling level of −0.6 dB while the maximum backward coupling occurs

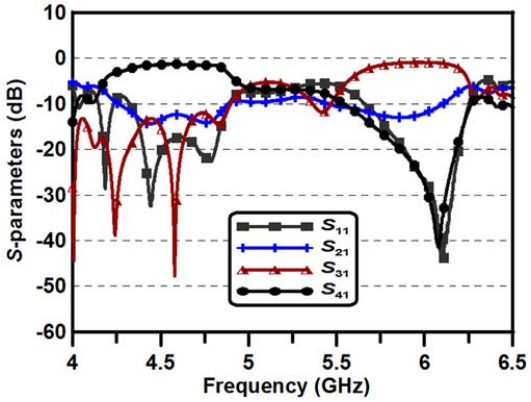

Fig. 14. Measured S-parameters of the proposed dual-band quasi-0-dB coupled-line coupler.

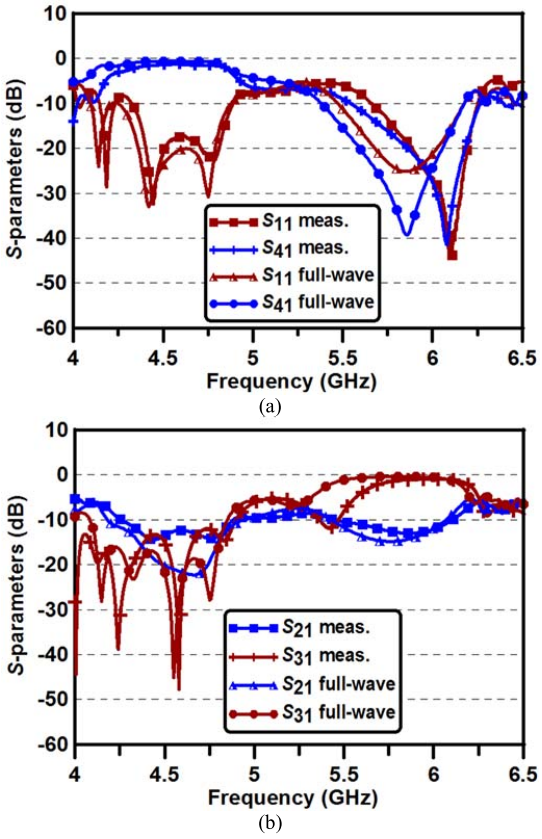

Fig. 15. Comparison between the full-wave simulated results and the experimental results. (a) S_{11} and S_{41}. (b) S_{21} and S_{31}.

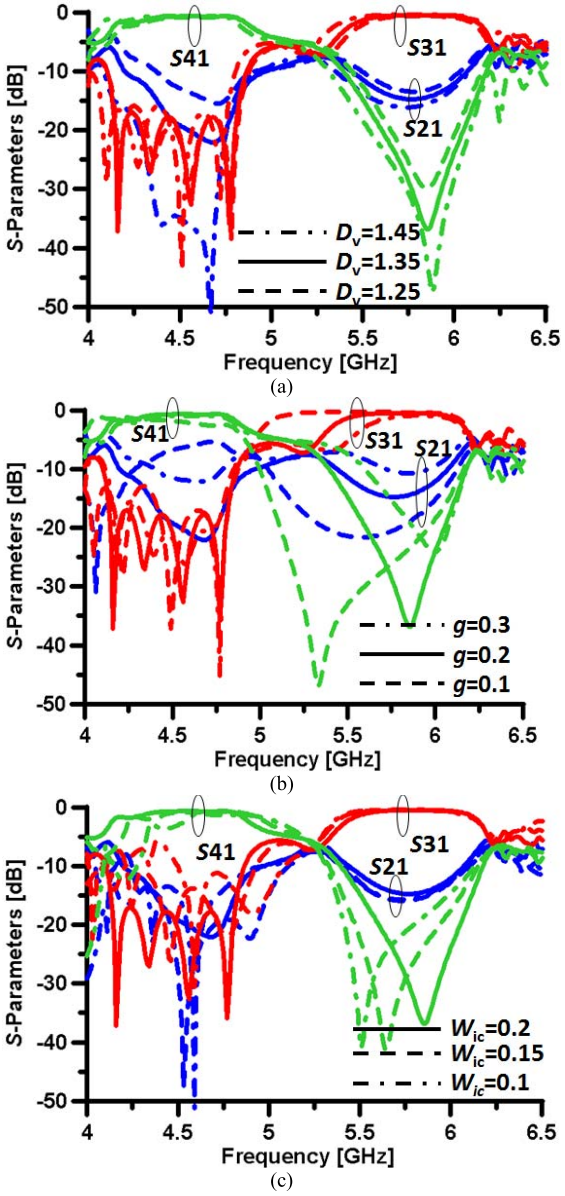

Fig. 16. Studies of the coupler sensitivity with respect to (a) via distance Dv, (b) coupling gap g, and (c) digit width $W_{\rm ic}$. All parameters are in mm.

at 5.8 GHz with a coupling level of −0.4 dB. The 3-dB bandwidths of the forward and backward coupling regions are from 4.1 to 4.93 GHz and from 5.37 to 6.18 GHz, corresponding to the fractional bandwidths of 18.4% and 14%, respectively. Moreover, the isolation bandwidths (for <-15 dB) are 15.7% and 10.9% in the lower and upper bands, respectively.

The proposed coupler was fabricated and shown in Fig. 1. The measured S-parameters are shown in Fig. 14 where dual quasi-0-dB couplings at frequencies of interest are validated. The maximum forward coupling level is −1.3 dB at 4.58 GHz with the 3-dB fractional bandwidth of 15.8%. The isolation bandwidth for $|S_{31}| < -15$ dB is 3.5%. Moreover, in the backward coupling region, the maximum coupling level is −0.9 dB at 5.94 GHz. The corresponding 3-dB bandwidth and isolation bandwidth are 10.8% and 8.5%, respectively. For easy comparison, the full-wave simulation and measurement results are superimposed in Fig. 15. The experimental results are in good agreement with the full-wave simulation results. In Fig. 15, it was observed that due to the upper shift of the frequency $\omega^o_{\rm sh}$, the lower end frequency of the backward coupling region, the coupling level $|S_{31}|$ and bandwidth are reduced in the backward coupling region. Furthermore, owing to the increase of $\omega^o_{\rm sh}$ with respect to $\omega^e_{\rm se}$ (the upper end frequency of the forward coupling region), the phase difference of the even and odd modes is thus altered, by which the complete coupling to port 4 is unable to satisfy and a portion

of the total power is delivered to port 2 in the forward coupling band. The performance deviation can be ascribed to the fabrication errors, including the over-etching effect and tolerance of via distance, the surface roughness effect, and the variations of the substrate thickness and dielectric constant. In particular, the coupler sensitivity was studied for the overall performance with respect to the via distance D_v, the coupling gap g, and the digit width $W_{\rm ic}$. Fig. 16 shows the performance variations and only the power levels of S_{21}, S_{31}, and S_{41} are shown here. Note that the variation step of 0.1 mm was chosen for D_v and g, and the step of 0.05 mm for $W_{\rm ic}$. Except the sweep parameter, the other dimensions are the same as the coupler dimensions shown in the caption of Fig. 6. It can be observed that the two operational bands are relatively sensitive to the gap g between the coupled lines, and the forward coupling (lower) band is more susceptible to parameter variations of D_v and $W_{\rm ic}$ when compared with the backward coupling (higher) band. Nevertheless, the experimental results demonstrate and validate the feasibility of the proposed design concept and approach to implementation of the dual-band quasi-0-dB coupled-line coupler based on the CRLH transmission lines.

V. Conclusion

A novel CRLH dual-band quasi-0-dB coupled-line coupler implemented by the complete forward and backward couplings at the lower and higher operational bands, respectively, is proposed and experimentally demonstrated. The detailed implementation approach and design considerations are discussed based on the even and odd-mode decomposition technique. By carefully engineering the even and odd-mode dispersion relations and Bloch impedances, the complete couplings in dual bands can be fulfilled in a simple single-layer structure.

References

[1] R. Mongia, I. Bahl, P. Bhartia, and J. Hong, *RF and Microwave Coupled-Line Circuits*. Norwood, MA, USA: Artech House, 2007.

[2] D. M. Pozar, *Microwave Engineering*, 2nd ed. New York, NY, USA: Wiley, 1998.

[3] X. Wang, W.-Y. Yin, and K.-L. Wu, "A dual-band coupled-line coupler with an arbitrary coupling coefficient," *IEEE Trans. Microw. Theory Tech.*, vol. 60, no. 4, pp. 945–951, Apr. 2012.

[4] C. Caloz and T. Itoh, *Electromagnetic Metamaterials: Transmission Line Theory and Microwave Applications*. New York, NY, USA: Wiley, 2005.

[5] T. Fujii and I. Ohta, "Size-reduction of coupled-microstrip 3 dB forward couplers by loading with periodic shunt capacitive stubs," in *IEEE MTT-S Int. Microw. Symp. Dig.*, Jun. 2005, pp. 1235–1238.

[6] C.-C. Chang, Y. Qian, and T. Itoh, "Enhanced forward coupling phenomena between microstrip lines on periodically patterned ground plane," in *IEEE MTT-S Int. Microw. Symp. Dig.*, May 2001, pp. 2039–2042.

[7] C. Caloz and T. Itoh, "A novel mixed conventional microstrip and composite right/left-handed backward-wave directional coupler with broadband and tight coupling characteristics," *IEEE Microw. Wireless Compon. Lett.*, vol. 14, no. 1, pp. 31–33, Jan. 2004.

[8] R. Islam and G. V. Eleftheriades, "A planar metamaterial co-directional coupler that couples power backwards," in *IEEE MTT-S Int. Microw. Symp. Dig.*, Jun. 2003, pp. 321–324.

[9] S.-G. Mao and M.-S. Wu, "A novel 3-dB directional coupler with broad bandwidth and compact size using composite right/left-handed coplanar waveguides," *IEEE Microw. Wireless Compon. Lett.*, vol. 17, no. 5, pp. 331–333, May 2007.

[10] C. Caloz, A. Sanada, and T. Itoh, "A novel composite right-/left-handed coupled-line directional coupler with arbitrary coupling level and broad bandwidth," *IEEE Trans. Microw. Theory Tech.*, vol. 52, no. 3, pp. 980–992, Mar. 2004.

[11] A. Hirota, Y. Tahara, and N. Yoneda, "A compact forward coupler using coupled composite right/left-handed transmission lines," *IEEE Trans. Microw. Theory Tech.*, vol. 57, no. 12, pp. 3127–3133, Dec. 2009.

[12] A. Hirota. Y. Tahara, and N. Yoneda, "A wide band forward coupler with balanced composite right-/left-handed transmission lines," in *IEEE MTT-S Int. Microw. Symp. Dig.*, Jun. 2011, pp. 1–4.

[13] L. Liu, C. Caloz, C.-C. Chang, and T. Itoh, "Forward coupling phenomena between artificial left-handed transmission lines," *J. Appl. Phys.*, vol. 92, no. 9, pp. 5560–5565, Nov. 2002.

[14] H. V. Nguyen and C. Caloz, "Generalized coupled-mode approach of metamaterial coupled-line couplers: Coupling theory, phenomenological explanation, and experimental demonstration," *IEEE Trans. Microw. Theory Tech.*, vol. 55, no. 5, pp. 1029–1039, May 2007.

[15] P. K. Ikalainen and G. L. Matthaei, "Wide-band, forward-coupling microstrip hybrids with high directivity," *IEEE Trans. Microw. Theory Tech.*, vol. 35, no. 8, pp. 719–725, Aug. 1987.

Pei-Ling Chi (S'08–M'11) received the B.S. and M.S. degrees in communication engineering from National Chiao-Tung University (NCTU), Hsinchu, Taiwan, in 2004 and 2006, respectively, and the Ph.D. degree in electrical engineering from the University of California at Los Angeles, Los Angeles, CA, USA, in 2011.

She has been with NCTU since 2011 as an Assistant Professor of electrical and computer engineering. She holds several U.S. and international patents in left-handed meta-materials. Her current research interests include the analysis and design of the left-handed meta-material circuits, implementation of microwave components and integrated systems, and development of mm-wave/THz antennas and communications.

Dr. Chi was a recipient of the Research Creativity Award from the National Science Council, Taiwan, in 2004.

Chun-Chih Liu, photograph and biography not available at the time of publication.